

NUMERICAL AND PHYSICAL MAGNETIC HELICITY PRODUCTION IN A KINEMATIC DYNAMO

AXEL BRANDENBURG^{1,2,3} & EVAN O'CONNOR²

¹Nordita, KTH Royal Institute of Technology and Stockholm University, Roslagstullsbacken 23, SE-10691 Stockholm, Sweden

²Department of Astronomy, AlbaNova University Center, Stockholm University, SE-10691 Stockholm, Sweden

³McWilliams Center for Cosmology & Department of Physics, Carnegie Mellon University, Pittsburgh, PA 15213, USA

(Revision: 1.28)

Draft version July 22, 2020

ABSTRACT

...
Subject headings: dynamo — magnetic fields — MHD — turbulence — methods: numerical

1. INTRODUCTION

Magnetic helicity is conserved by the magnetohydrodynamic (MHD) equations in the limit of large magnetic Reynolds numbers. This is a remarkable property of MHD, because something analogous does not exist for the kinetic helicity, which does change—even when the Reynolds number is very large. When the flow is forced with a helical forcing function, it leads to an efficient dynamo process. Since magnetic helicity is conserved, the magnetic field tends to become bihelical with opposite signs of magnetic helicity at large and small length scales, whose contributions cancel.

Numerical codes tend to obey magnetic helicity conservation reasonably well when magnetic energy and helicity dissipation is accomplished through Ohm's law by microphysical resistivity (Brandenburg & Scannapieco 2020). Magnetic energy dissipation through purely numerical means, on the other hand, yields a magnetic helicity evolution that strongly depends on the details of the numerical scheme. With the eight-wave solver of the FLASH code, for example, spurious magnetic helicity is generated both over long and short time scales (Brandenburg & Scannapieco 2020). By contrast, the SPARK solver in FLASH produces much less spurious magnetic helicity, as will be demonstrated here in detail.

At finite magnetic Reynolds numbers, some level of magnetic helicity is always generated. There has been significant progress in characterizing magnetic helicity production during the late evolution of the dynamo process in its saturation phase (Brandenburg 2001; Field & Blackman 2002; Blackman & Brandenburg 2002), but not much is known about the early evolution before non-linear effects have played a role. An exception is the work of Brandenburg et al. (2002), who found that for the ABC flow, the normalized magnetic helicity decreases with magnetic Reynolds number Re_M like $\text{Re}_M^{-1/2}$; see their Figure 5. Assuming Re_M to be proportional to the number of mesh points N , this suggests a relatively slow convergence with increasing resolution. It turns out, however, that the actual magnetic helicity produced decreases faster—approximately like $N^{-3/2}$. Investigating and understanding this in detail is the purpose of the present work.

2. DEFINITION OF THE MODEL

The evolution of the magnetic field \mathbf{B} is governed by the induction equation,

$$\frac{d\mathbf{B}}{dt} = \nabla \times (\mathbf{U} \times \mathbf{B} - \eta \mathbf{J}), \quad (1)$$

where $\mathbf{U}(\mathbf{x}, t)$ is the velocity field, which is in general time-dependent, $\mathbf{J} = \nabla \times \mathbf{B}/\mu_0$ is the current density, with μ_0 being the vacuum permeability, and η is the magnetic diffusivity. The mean magnetic energy density is given by $\langle \mathbf{B}^2 \rangle / 2\mu_0$, where angle brackets denote volume averaging. A more convenient quantity is the mean squared magnetic field,

$$\mathcal{M} = \langle \mathbf{B}^2 \rangle, \quad (2)$$

as well as the magnetic and normalized current helicities

$$\mathcal{H} = \langle \mathbf{A} \cdot \mathbf{B} \rangle \quad \text{and} \quad \mathcal{C} = \nu_0 \langle \mathbf{J} \cdot \mathbf{B} \rangle. \quad (3)$$

We consider a periodic domain of size L^3 , so the smallest wavenumber is $k_1 = 2\pi/L$. Because of periodicity, there are no magnetic helicity fluxes and the mean magnetic helicity density $\langle \mathbf{A} \cdot \mathbf{B} \rangle$ is governed by the equation

$$\frac{d}{dt} \langle \mathbf{A} \cdot \mathbf{B} \rangle = -2\eta \langle \mathbf{J} \cdot \mathbf{B} \rangle \quad (4)$$

During the kinematic dynamo phase of interest, the rms magnetic field increases exponentially with the growth rate λ and the mean squared magnetic field $\langle \mathbf{B}^2 \rangle$ grows at a rate 2λ . It is then useful to introduce normalized quantities

$$\epsilon_M = k_1 \langle \mathbf{A} \cdot \mathbf{B} \rangle / \langle \mathbf{B}^2 \rangle, \quad k_C = \langle \mathbf{J} \cdot \mathbf{B} \rangle / \langle \mathbf{B}^2 \rangle, \quad (5)$$

where ϵ_M is non-dimensional and characterizes the net magnetic helicity in the system, and k_C has the units of a wavenumber that characterizes the magnetic energy spectrum. We then have

$$2\lambda \epsilon_M = -2\eta k_C k_1 \quad (\text{kinematic phase}). \quad (6)$$

Thus, we see that $\epsilon_M < 0$, when the magnetic field grows ($\lambda > 0$). It is conceivable that k_C increases with Re_M to some power n , so we write $k_C = k_1 \text{Re}_M^n$, where n is an empirically determined parameter. For Kolmogorov turbulence, for example, one expects $n = 1/4$ (Blackman & Brandenburg 2002). In general, however, we have

$$\epsilon_M = -\eta k_C k_1^2 / \lambda = -\tilde{\lambda}^{-1} \tilde{k}_f^{-2} \text{Re}_M^{-(1-n)}, \quad (7)$$

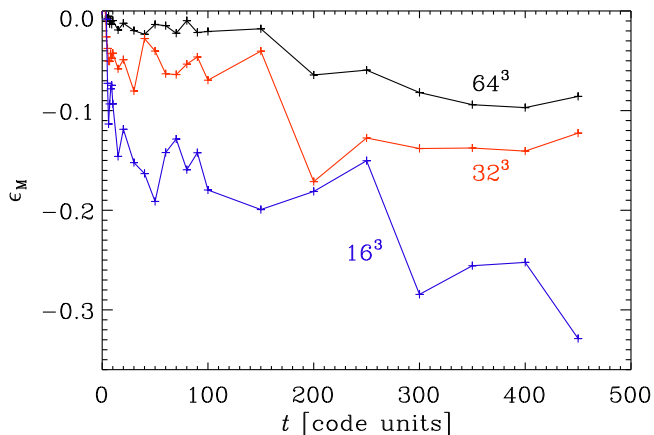


FIG. 1.— FLASH .

where $\tilde{\lambda} = \lambda/u_{\text{rms}}k_f$ is the nondimensional growth rate and $\tilde{k}_f = k_f/k_1$ is the nondimensional forcing wavenumber. The findings of Brandenburg et al. (2002) are reproduced when $n = 1/2$. In an ideal code, we expect there to be an effective magnetic Reynolds number proportional to N , so we define

$$R_{\text{eff}} = R_0 N, \quad (8)$$

where R_0 is the mesh Reynolds number. We have dropped here the specification to the *magnetic* Reynolds number, because for ideal codes one expects the fluid and magnetic Reynolds numbers to be the same. The empirical finding $\epsilon_M \propto N^{-3/2}$ then implies then for n a negative value, $n = -1/2$, and thus

$$\epsilon_M = -\tilde{\lambda}^{-1} R_{\text{eff}}^{-3/2}. \quad (9)$$

This allows us to compute the effective grid Reynolds number as

$$R_0 = -N^{-1} (\tilde{\lambda} \tilde{k}_f^2 \epsilon_M)^{-2/3}. \quad (10)$$

Figure 1 shows magnetic helicity production with the SPARK solver in FLASH. The early exponential growth phase of the dynamo corresponds to the time interval from 20 to 140 (in code units). In the following, we average the instantaneous growth rate, $\lambda(t) = d \ln B_{\text{rms}}/dt$ and various other normalized quantities such as ϵ_M and k_C , as well as u_{rms} , over this time interval. Figure 2 shows that the magnetic helicity production decreases with increasing resolution N like $N^{-1.5}$. (Not clear why.)

In Figure 3 we show the magnetic helicity evolution in DNS for different values of Re_M ; see also Table 1 for a summary of quantities averaged over the linear growth phase. The data of the DNS correspond to an inhomogeneous dataset because both Pr_M and Re_M vary. We also note that in the DNS, u_{rms} is only about half the value used in the FLASH code results. Figure 4 shows that the magnetic helicity production decreases with Re_M like $\text{Re}_M^{-0.7}$, at least for the range of values shown here.

In Figure 5 we combine the FLASH and PENCIL CODE results. For each value of Re_M , we show here separate lines with different resolutions.

Using Equation (10), we compute R_0 , which is shown in Figure 7 as a function of N .

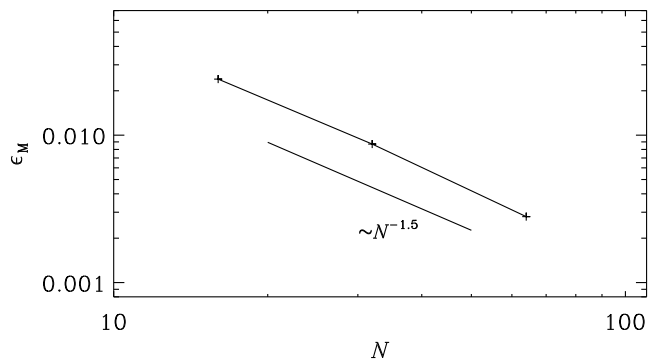


FIG. 2.— Results with FLASH .

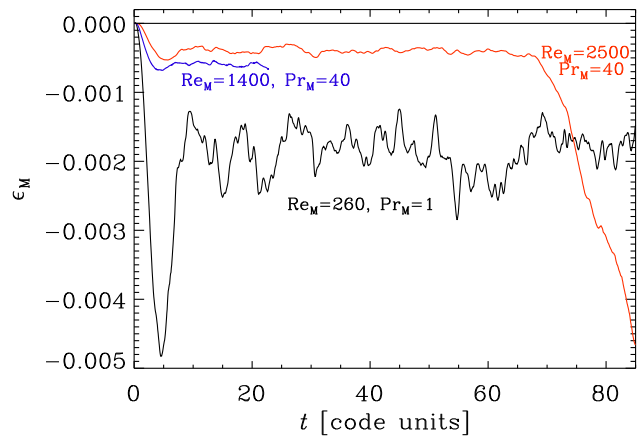


FIG. 3.— Results with PENCIL CODE.

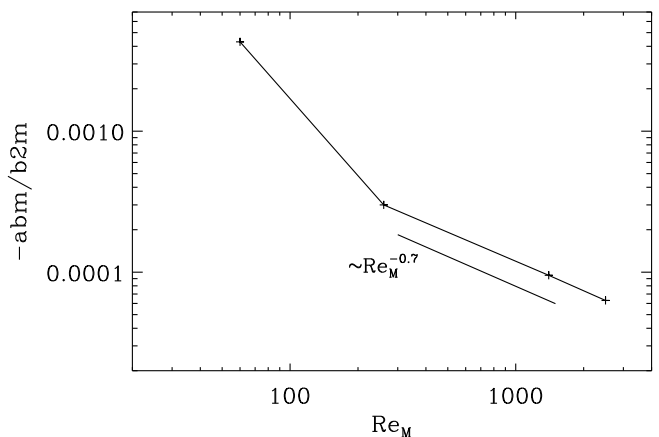


FIG. 4.— Results with PENCIL CODE.

Looking at Table 1, we see that k_C/k_f converges with N more slowly than ϵ_M .

3. TWO-SCALE APPROACH

In a closed or periodic domain, magnetic helicity can only be produced by the $\langle \mathbf{J} \cdot \mathbf{B} \rangle$ term, even if $\langle \mathbf{A} \cdot \mathbf{B} \rangle = 0$ initially. To understand this, we now compute $\langle \mathbf{J} \cdot \mathbf{B} \rangle$

TABLE 1
FLASH (FIRST THREE ROWS) AND PENCIL CODE RESULTS.

Run	N	k_f	u_{rms}	ν	η	Pr_M	Re	Re_M	$-\epsilon_M$	k_C/k_1	λ
O	16	16.5	0.405	0	0	–	–	–	2.4e-02	-2.5e-01	7.8e-02
O	32	16.5	0.427	0	0	–	–	–	8.7e-03	4.8e-02	1.2e-01
O	64	16.5	0.408	0	0	–	–	–	2.8e-03	5.4e-02	1.3e-01
I	128	16.5	0.211	5.0e-05	5.0e-05	1	255.3	255.3	3.5e-04	9.4e-01	2.0e-01
I	256	16.5	0.212	5.0e-05	5.0e-05	1	256.5	256.5	3.1e-04	1.1e+00	1.9e-01
I	512	16.5	0.211	5.0e-05	5.0e-05	1	255.8	255.8	3.0e-04	1.1e+00	1.9e-01
P	256	16.5	0.206	2.0e-04	5.0e-06	40	62.5	2501.7	5.8e-05	6.2e-01	3.5e-01
P	512	16.5	0.206	2.0e-04	5.0e-06	40	62.3	2493.6	6.3e-05	4.2e+00	3.5e-01
X	64	28.3	0.085	2.0e-03	5.0e-05	40	1.5	59.8	4.3e-03	1.2e+01	1.5e-01
X	128	28.3	0.085	2.0e-03	5.0e-05	40	1.5	60.1	4.1e-03	1.3e+01	1.6e-01
X	256	28.3	0.084	2.0e-03	5.0e-05	40	1.5	59.6	4.3e-03	1.3e+01	1.5e-01
Y	128	28.3	0.178	4.0e-04	1.0e-05	40	15.7	629.0	1.3e-04	-2.7e+00	4.0e-01
Y	256	28.3	0.180	4.0e-04	1.0e-05	40	15.9	635.6	2.8e-04	9.5e+00	3.8e-01
Y	512	28.3	0.180	4.0e-04	1.0e-05	40	15.8	634.0	2.7e-04	1.0e+01	3.8e-01
Z	128	28.3	0.194	2.0e-04	5.0e-06	40	34.3	1372.4	8.1e-05	-7.7e+00	1.4e+00
Z	256	28.3	0.199	2.0e-04	5.0e-06	40	35.2	1407.5	8.0e-05	5.1e-01	4.9e-01
Z	512	28.3	0.199	2.0e-04	5.0e-06	40	35.2	1407.7	9.3e-05	8.6e+00	4.9e-01
Z	1024	28.3	0.196	2.0e-04	5.0e-06	40	34.5	1380.9	9.5e-05	9.3e+00	4.9e-01

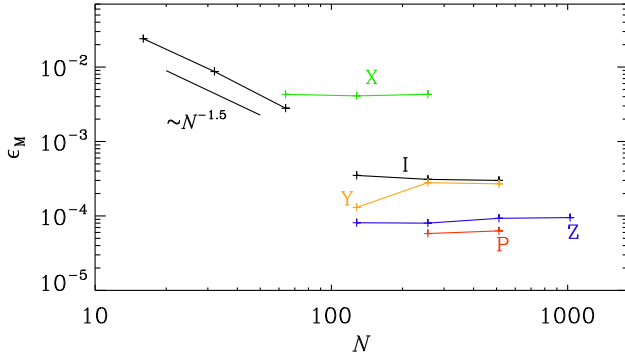


FIG. 5.— Combined presentation of the results both with FLASH and the PENCIL CODE.

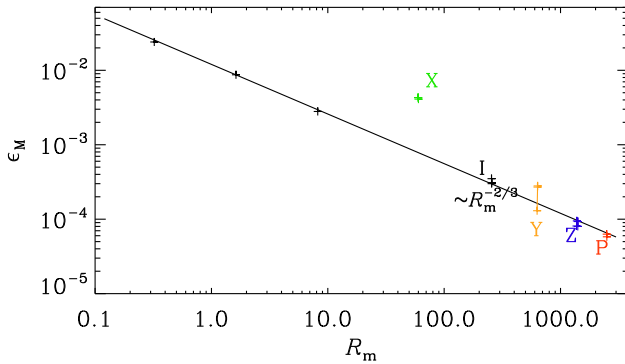


FIG. 6.— Combined presentation of the results both with FLASH and the PENCIL CODE versus Re_M . For the FLASH results, we have assumed $\text{Re}_M = N^{7/3}/2000$.

under the two-scale approximation, i.e.,

$$\langle \mathbf{J} \cdot \mathbf{B} \rangle = \langle \bar{\mathbf{J}} \cdot \bar{\mathbf{B}} \rangle + \langle \mathbf{j} \cdot \mathbf{b} \rangle \quad (11)$$

$$\langle \mathbf{J} \cdot \mathbf{B} \rangle = k_1^2 \langle \bar{\mathbf{A}} \cdot \bar{\mathbf{B}} \rangle + k_f^2 \langle \mathbf{a} \cdot \mathbf{b} \rangle \quad (12)$$

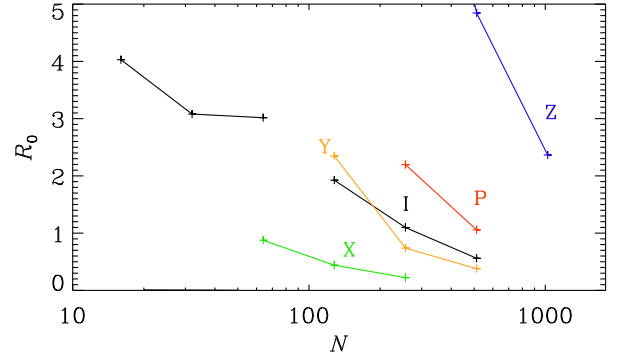


FIG. 7.— Effective grid Reynolds number. (Dubious?)

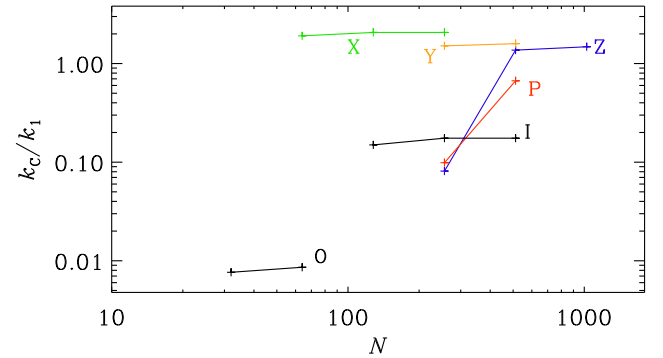


FIG. 8.— Dependence of k_C on N .

Making use of $\mathcal{H}_M = \langle \bar{\mathbf{A}} \cdot \bar{\mathbf{B}} \rangle + \langle \mathbf{a} \cdot \mathbf{b} \rangle$, we have $\langle \bar{\mathbf{A}} \cdot \bar{\mathbf{B}} \rangle = \mathcal{H}_M - \langle \mathbf{a} \cdot \mathbf{b} \rangle$, so

$$\langle \mathbf{J} \cdot \mathbf{B} \rangle = k_1^2 (\mathcal{H}_M - \langle \mathbf{a} \cdot \mathbf{b} \rangle) + k_f^2 \langle \mathbf{a} \cdot \mathbf{b} \rangle \quad (13)$$

$$\langle \mathbf{J} \cdot \mathbf{B} \rangle = k_1^2 \mathcal{H}_M + (k_f^2 - k_1^2) \langle \mathbf{a} \cdot \mathbf{b} \rangle \quad (14)$$

$$\frac{d}{dt} \langle \mathbf{A} \cdot \mathbf{B} \rangle = -2\eta \langle \mathbf{J} \cdot \mathbf{B} \rangle \quad (15)$$

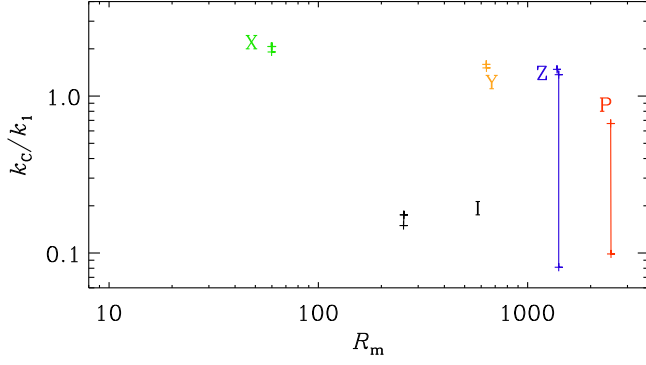


FIG. 9.— Dependence of $k_c Q$ on Re_M .

$$\frac{d\mathcal{H}_M}{dt} = -2\eta\mathcal{H}_M - 2\eta(k_f^2 - k_1^2)\langle \mathbf{a} \cdot \mathbf{b} \rangle \quad (16)$$

Using $k_f^2\langle \mathbf{a} \cdot \mathbf{b} \rangle \approx \langle \mathbf{j} \cdot \mathbf{b} \rangle \approx \mu_0\rho_0\langle \boldsymbol{\omega} \cdot \mathbf{u} \rangle$, we have

$$\frac{d\mathcal{H}_M}{dt} = -2\eta\mathcal{H}_M - 2\eta(1 - k_1^2/k_f^2)\mu_0\rho_0\langle \boldsymbol{\omega} \cdot \mathbf{u} \rangle \quad (17)$$

4. CONCLUSIONS SO FAR

The magnetic helicity produced during the early kinematic phase of a dynamo is being reduced with increasing resolution. Both SPARK and the PENCIL CODE reduce the magnetic helicity production approximately like $N^{-1.5}$.

REFERENCES

- Blackman, E. G., & Brandenburg, A. 2002, ApJ, 579, 359
 Brandenburg, A. 2001, ApJ, 550, 824
 Brandenburg, A., & Scannapieco, E. 2020, ApJ, 889, 55
 Brandenburg, A., Dobler, W., & Subramanian, K. 2002, AN, 323, 99
 Field, G. B., & Blackman, E. G. 2002, ApJ, 572, 685